

# JOURNAL OF RADIATION EFFECTS

Research and Engineering

## Incorporation of Drift Loss Cone Effects on the Trapping of an Artificial Radiation Belt into LANL's Modeling Capability

G.S. Cunningham and M.M. Cowee

This paper was presented at the 33rd Annual HEART Technical Interchange Meeting  
Monterey, CA, April 5 – 8, 2016.

Prepared by AECOM for the HEART Society under contract to NSWC Crane.

## INCORPORATION OF DRIFT LOSS CONE EFFECTS ON THE TRAPPING OF AN ARTIFICIAL RADIATION BELT INTO LANL'S MODELING CAPABILITY

G.S. Cunningham and M.M. Cowee  
Los Alamos National Laboratory  
Los Alamos, NM

### Abstract

*Los Alamos National Laboratory has developed an end-to-end model that quantifies the total ionizing dose that a shielded component on a space asset will accrue due to interactions with trapped beta-decay electrons produced after a high-altitude nuclear explosion. The model consists of three major components: initial trapping, spatio-temporal evolution of the trapped population, and interaction of the evolving trapped population with a space asset to produce total ionizing dose. The initial trapping module calculates the fraction of betas produced by radioactive decay of nuclear fission products that will be trapped in the magnetic field surrounding Earth for at least one drift around Earth. Previously, the initial trapping calculation assumed a centered dipole magnetic field model whereas we know that Earth's magnetic field is offset from its geographic center and has higher-order non-dipole terms. Both the offset and the higher-order terms are captured in the International Geomagnetic Reference Field (IGRF) internal field model. In a centered dipole, the electrons that are trapped on a magnetic field line at one longitude will be trapped at all other longitudes as they drift around Earth due to azimuthal symmetry of the field, but the offset and higher-order terms of the IGRF field affects the drift of the trapped electrons and causes some that are trapped at one longitude to be lost at other longitudes. These electrons are called "quasi-trapped" and are said to be in the drift loss cone since they will be lost during their first drift around Earth. In this paper we report on the effect of incorporating the drift of electrons around Earth using the IGRF field on the trapping fraction as compared to using a centered dipole. We find that the new, more accurate, methodology produces higher trapping fractions for bursts above the South Atlantic Anomaly, a region of low magnetic field strength, and lower trapping fractions for bursts in regions with higher magnetic field strength than expected from a centered dipole.*

### Introduction

The high altitude nuclear test shots of the 1950's and 60's demonstrated that high energy beta-decay electrons (betas), produced by radioactive decay of fission fragments, can become trapped in Earth's magnetic field and form an artificial radiation belt or enhance a pre-existing natural belt [1]. Los Alamos National Laboratory (LANL) has developed an end-to-end model that quantifies the total ionizing dose that a shielded component on a space asset will accrue due to interactions with such radiation belts. The LANL end-to-end model consists of three major components: initial trapping, spatio-temporal evolution of the trapped population, and interaction of the evolving trapped population with a shielded component on a space asset to produce total ionizing dose. The initial trapping is computed by the Electron Source Model (ESM). The ESM uses a fission fragment debris model

that allows some of the debris to travel along field lines, emitting electrons isotropically along the way. Electrons that have velocity vectors that are nearly parallel to the local magnetic field line direction will travel down the field line to the near-surface atmosphere and be lost, whereas electrons that have velocity vectors nearly perpendicular to the field direction will "mirror" in the field and be trapped. The gradient and curvature of the magnetic field cause the electrons to drift around Earth. We have recently improved the ESM so that it can make use of the International Geomagnetic Reference Field (IGRF), which includes the tilt and offset of the dipole portion of the field as well as the higher-order terms that can be modeled as a sum of spherical harmonics whose coefficients vary slowly with time, whereas the ESM previously assumed that the surrounding magnetic field was a centered dipole [2]. Furthermore, we also now compute a

---

This work was sponsored by the Defense Threat Reduction Agency under contract DTR10027-11230.

---

(Distribution Statement A: Approved for Public Release. Los Alamos National Laboratory Unclassified Report LA-UR-16-23823.)

complete set of closed drift-shells, i.e., drift trajectories for which the electron's minimum altitude is above 120 km at all longitudes and can therefore assume to be trapped for at least one drift around Earth (longitudinal drift is caused by the gradient and curvature of the magnetic field and takes on the order of 10's of minutes for an MeV electron). Combining the two new capabilities allows us to compute the effect of drifting in an IGRF field on the trapping fraction, which we report on here.

First, we review the basic particle motions in a magnetic field and their associated invariants. Next we discuss the new capability that has been introduced into the ESM, the calculation of the drift shells, and the mapping of the electrons produced by the ESM onto the set of closed drift shells. Finally, we compare the trapping fractions obtained under various assumptions and draw some conclusions.

## Background

Charged particles with a velocity  $\vec{v}$  in a magnetic field  $\vec{B}$  undergo three periodic motions: gyration about a magnetic field line due to the Lorentz  $q\vec{v} \times \vec{B}$  force, movement along a magnetic field line due to the component of velocity that is parallel to the magnetic field vector (with "mirroring" at some altitude due to conservation of the 1st invariant, discussed in the next paragraph), and drift around Earth due to the gradient and curvature of the magnetic field. Associated with each periodic motion is an adiabatic invariant that is conserved so long as there are no collisions and variations in the electric or magnetic field occur on time scales that are long compared to the periodic motion.

The gyro motion is associated with the first adiabatic invariant  $\mu = p^2 \sin^2(\alpha)/(2m_0 B)$ , where  $p$  is the total momentum,  $\alpha$  is the local pitch-angle, i.e., the angle of the velocity vector with respect to the magnetic field direction,  $m_0$  is mass, and  $B$  is magnetic field intensity. Conservation of  $\mu$  as a particle moves along a field line toward the mirror point implies that  $\alpha$  increases until all of the momentum is perpendicular to the field line, i.e.,  $\alpha = 90^\circ$ , at which point the particle begins to travel in the opposite direction. Since  $\alpha$  varies along the field line, the value of  $\alpha$  at the point where the intensity of the magnetic field is minimized is often used and is called

the equatorial pitch-angle,  $\alpha_{eq}$ , since the magnetic field intensity is minimized along any field line at the magnetic equator for a dipole field.

The bounce motion is associated with the second adiabatic invariant,  $J = 2 \int_{s_m}^{n_m} p \cos(\alpha) ds$ , where  $s_m$  is the arclength associated with the southern hemisphere mirror point and  $n_m$  is the arclength associated with the northern hemisphere mirror point. We use a related version of the invariant  $K = \sqrt{B_m} I = \int_{s_m}^{n_m} \sqrt{B_m - B(s)} ds$ , where  $B(s_m) = B(n_m) = B_m$  is the mirror-point magnetic field intensity and is also an invariant of motion under the assumption that the total momentum doesn't change.

As the particle drifts longitudinally around Earth, it drifts onto field lines that preserve the first two invariants, or equivalently,  $B_m$  and  $K$ . At each longitude there is a unique field line with one minimum value that has the particle's  $B_m$  and  $K$ . The set of field lines that have this property are called the drift-shell of the particle. If we trace the field lines to 120 km altitude in the northern hemisphere, the set of points defines a contour  $\pi$  inside of which we can integrate the magnetic flux that points outward,  $\Phi = \int_{\pi} \vec{B} \cdot d\vec{S}$ . The quantity  $\Phi$  is an invariant of motion associated with the drift motion of the particle. A related quantity that we use is the Roederer  $L^* = 2\pi B_E R_E^2 / \Phi$  [3]. If the magnetic field is a centered dipole, then  $r(\theta) = L \sin^2(\theta)$  defines the field lines and  $L^* = L$ , where  $\theta$  is the polar angle from the north magnetic pole, also called the colatitude. The approach that we use to compute the drift-shells, also used for the results presented in this paper, is detailed in [4].

In a centered dipole, the value of  $\alpha_{eq}$  for a particle that mirrors at the 120 km atmosphere cutoff altitude is called the bounce loss cone angle  $\alpha_{blc}$ . Particles that have a value of  $\alpha_{eq} < \alpha_{blc}$  will mirror below 120 km and are likely to be scattered and lost through collisions. We use 120 km as a simplification; in reality, the altitude at which particles are scattered and lost to the atmosphere is energy-dependent, with higher energy particles able to reach lower altitudes. We note that for  $L < 1.0188$ , the particle's entire orbital path is below 120 km altitude and so  $\alpha_{blc} = 90^\circ$ .

In an eccentric dipole, i.e., one that is offset and tilted relative to Earth's rotation axis, the dipole field lines are azimuthally symmetric about the axis of the dipole, but are shifted and rotated relative to Earth's rotation axis. Thus, the value of  $\alpha_{blc}$  depends on longitude. Because  $\alpha_{eq}$  is a conserved quantity in a dipole, the maximum value of  $\alpha_{blc}$  over all longitudes,  $\alpha_{dlc} = \max_{\varphi} \{\alpha_{blc}(\varphi)\}$ , called the drift loss cone, is more relevant to the trapping fraction since it defines the set of equatorial pitch-angles that will remain trapped over an entire drift orbit around Earth. One can analytically calculate  $\alpha_{dlc}$  as a function of  $L$  and compare it to  $\alpha_{blc}$  for the centered dipole (Fig. 1). Similarly, one can compute  $\alpha_{dlc}$  for the IGRF magnetic field model (circa 1960), although it is important to note that  $\alpha_{eq}$  is not a conserved quantity in a non-dipole field and therefore the  $\alpha_{eq}$  that is plotted in Fig. 1 for the IGRF model is technically only valid at a single longitude. A more precise statement for the IGRF model would be to plot the maximum value of the second invariant,  $K$ , for which a closed drift-shell exists; however, we chose not to do this because the dependence of  $\alpha_{eq}$  on longitude is relatively weak in Fig. 1 (less than a degree).

## Methodology

Note that if one were to assume that particles start to interact strongly with the atmosphere at 500 km altitude and thus become lost if they continue to travel along the field line below that point, then the plot of  $\alpha_{blc}$  vs  $L$  for a centered dipole in Fig. 1 (the red line) would be shifted to the right and look more like the plots of  $\alpha_{dlc}$  using the

eccentric dipole (blue line) and IGRF 1960 (black line). For this reason, because we were constrained to use a centered dipole field model in our previous work, we used a 500 km cutoff for the mirror point of trapped electrons to mimic the drift loss cone effect when calculating the trapping fraction using the ESM. The present work compares this approach for calculating trapping fractions to two other approaches.

The first approach uses the value of  $\alpha_{blc}$  for the field lines on which the beta-decay electrons are initially produced. The second approach maps the bounce-trapped electrons onto drift-shells and computes the trapping fraction as the number of electrons that are trapped for at least one orbit around Earth divided by the total number of electrons produced. In previous work [4], we detail how we construct a comprehensive set of drift-shells that consist of field lines with a single minimum value. There may be closed drift-shells that have field lines with more than one minimum value, called Shabansky-type orbits [5], but we do not consider these orbits since they only occur at larger  $L$  and it is not clear that electrons on these orbits would stay trapped for very long [6]. Each drift-shell is associated with a pair of second and third invariants,  $(K_i, L_j^*)$ , and consists of a set of field lines sampling a discrete set of azimuths. The minimum value of the field intensity along each field line is associated with a radius and azimuth pair,  $(r_{ijk}, \varphi_{ijk})$ , at which point we compute the equatorial pitch-angle,  $\alpha_{ijk}^{eq}$ .

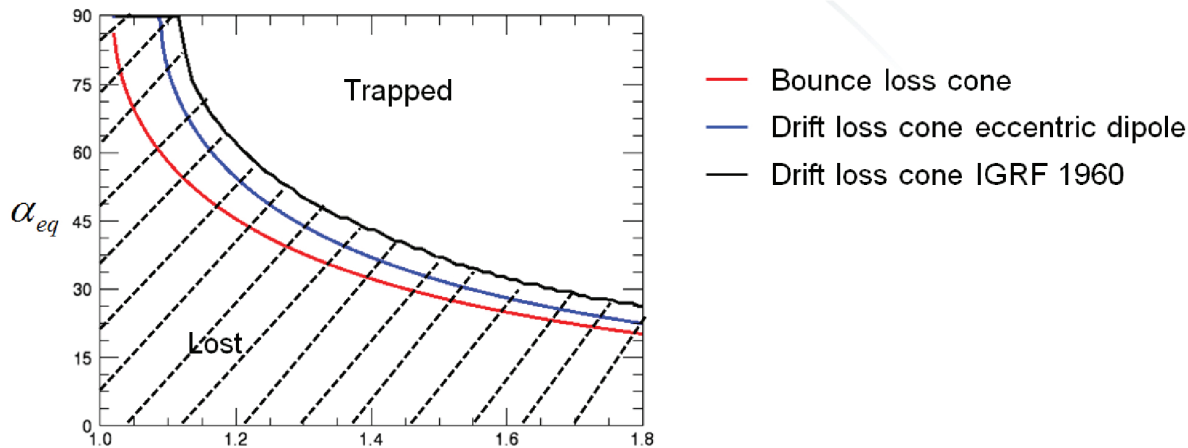


**Figure 1.** The bounce loss cone angle  $\alpha_{blc}$  for the centered dipole (red), drift loss cone angle  $\alpha_{dlc}$  for the eccentric dipole (blue) and drift loss cone angle  $\alpha_{dlc}$  for the IGRF 1960 magnetic field model (black) as a function of  $L$ .

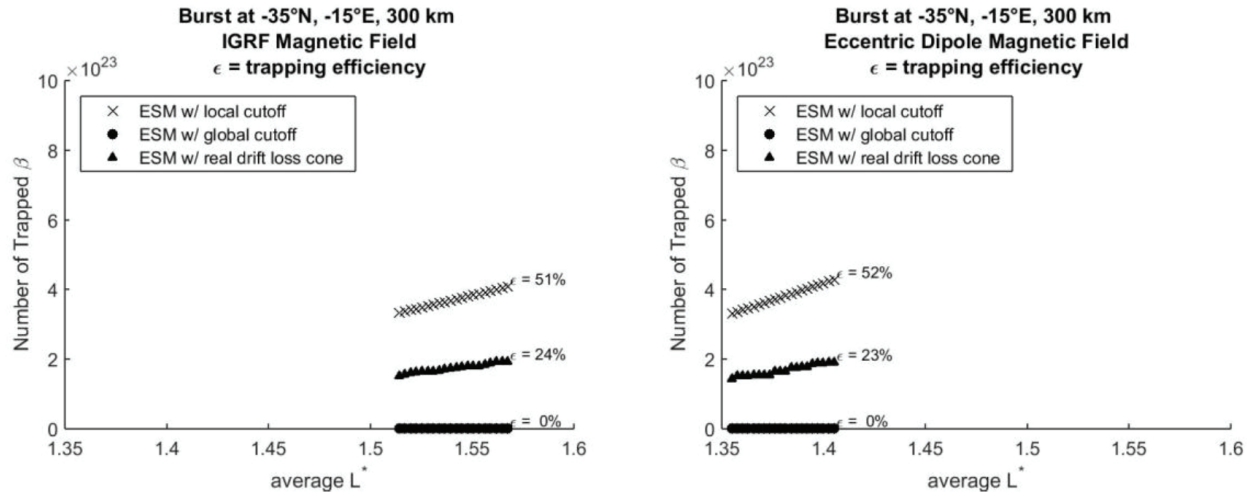


**Figure 2.** Total number of trapped electrons versus  $L^*$  using the eccentric dipole (right) and IGRF (left) magnetic field models, for a burst above the South Atlantic Anomaly at 300 km altitude. Trapping fractions were computed using a) the local bounce loss cone with 120 km atmosphere (x), b) the local bounce loss cone with 500 km atmosphere (circle), and c) by identifying those electrons that are on closed drift shells (triangles).

The ESM outputs the number of electrons in each of the equatorial pitch-angle bins for each of the field lines along which the fission fragment debris streams and produces isotropically distributed electrons at the point of production. The electrons are assumed to have a Carter-Reines distribution in energy [7]. Thus, the ESM output, integrated over energy, can be represented as  $N(\tilde{\alpha}_m^{eq}, \tilde{r}_n, \tilde{\varphi}_n)$ , where  $m$  indexes over pitch-angle and  $n$  indexes over field line. Note that  $N$  is not the number density, but the number density could be obtained by dividing  $N$  by an appropriate coordinate volume occupied by the particles in a given drift-shell. For each  $(\tilde{\alpha}_m^{eq}, \tilde{r}_n, \tilde{\varphi}_n)$  we first find a pair of bracketing closed drift-shells such that  $(\tilde{r}_n, \tilde{\varphi}_n)$  is in the domain of a bilinear map of the unit square onto the four points that come from field lines at neighboring azimuths from each drift shell and neighboring indices into  $L^*$  at fixed azimuths, i.e.,  $(r_{i,j,k}, \varphi_{i,j,k})$ ,  $(r_{i,j,k+1}, \varphi_{i,j,k+1})$ ,  $(r_{i,j+1,k}, \varphi_{i,j+1,k})$ , and  $(r_{i,j+1,k+1}, \varphi_{i,j+1,k+1})$ . Next, we use the same bilinear map to interpolate the  $\alpha_{ijk}^{eq}$  at the four corners to provide an estimate of  $\alpha_{eq}$  at each of two neighboring indices into  $K$  to ensure that  $\tilde{\alpha}_m^{eq}$  is bracketed by these values. If these two types of brackets exist, then we say that the electrons  $N(\tilde{\alpha}_m^{eq}, \tilde{r}_n, \tilde{\varphi}_n)$  have been mapped to a drift shell and are thus included in the population that is called “permanently trapped” meaning that the electrons

can drift around Earth without hitting the atmosphere at 120 km.

We used the ESM to produce  $N(\tilde{\alpha}_m^{eq}, \tilde{r}_n, \tilde{\varphi}_n)$  for two field models, eccentric dipole and IGRF 1960, for a variety of latitude, longitudes and altitudes (Table 1) intended to quantify the importance of including the drift loss cone in calculating trapping fractions. The IGRF 1960 internal field model was added to the TsyganenkoT89 [8] external field model, which should not have much affect at low  $L$ . For each ESM run, we computed three trapping fractions. First, we summed  $N(\tilde{\alpha}_m^{eq}, \tilde{r}_n, \tilde{\varphi}_n)$  over all bins such that  $\tilde{\alpha}_m^{eq} > \alpha_{blc}$  is satisfied for each sub-population of electrons on a given field line, and divided this number by  $N_{total}$ , the total number of electrons that are produced

**Table 1.** ESM scenarios and trapping fractions (percent) for the three approaches.

Lat	Lon	Alt	Offset dipole			IGRF 1960		
			Bounce	500 km	DLC	Bounce	500 km	DLC
0	0	400	46	24	17	40	12	2
0	0	800	66	53	50	57	41	27
0	90	400	51	24	4			
0	90	800	67	53	22	66	50	9
-35	-15	300	52	0	23	51	0	24
-35	-15	500	57	22	23	55	22	23
-35	-15	700	61	40	22	58	40	22
-35	-15	1000	68	56	24	64	54	24
35	165	300	53	33	16	52	31	13
35	165	500	59	37	16	59	39	14
35	165	1000	70	58	21	68	57	18

through radioactive decay of fission fragment debris. This trapping fraction is listed in the column labeled "Bounce." Second, we summed  $N(\tilde{\alpha}_m^{eq}, \tilde{r}_n, \tilde{\varphi}_n)$  over all bins such that  $\tilde{\alpha}_m^{eq} > \alpha_{blc}^{500}$  is satisfied for the field line on which the electrons are tied, where  $\alpha_{blc}^{500}$  is the bounce loss cone assuming that the atmosphere is at 500 km instead of 120 km, and divided this sum by  $N_{total}$  to get the trapping fractions in the column labeled 500 km in Table 1. Third, we attempted to find bracketing drift-shells as described above for each bin ( $m, n$ ) and summed  $N(\tilde{\alpha}_m^{eq}, \tilde{r}_n, \tilde{\varphi}_n)$  for those  $(m, n)$  where we successfully found a bracket and can thus assign the electrons in this sub-population to a closed drift-shell. We then divided this sum by  $N_{total}$  to get a third trapping fraction, labeled DLC in Table 1.

## Results

Proper inclusion of the drift loss cone is important when the burst is above the South Atlantic Anomaly (SAA), where the magnetic field is especially weak, as illustrated in Fig. 2. In this case, because the burst location is near the equator and at low altitude (300 km), every field line containing electrons in this case is entirely below 500 km, and so the trapping fraction computed using a bounce loss cone with altitude=500 km, as we did previously, is 0%. However, because the magnetic field intensity is weak in this area, the parti-

cles produced on these field lines will move away from Earth's surface as they drift and will be associated with closed drift shells. The trapping fraction computed by identifying which electrons are on closed drift shells is 24%, with little difference between results obtained using an eccentric dipole field model versus using IGRF 1960.

At other longitudes, as in Fig. 3, we find that the method for calculating trapping fraction based on using a bounce loss cone with the atmosphere at 500 km altitude grossly over-estimates the trapping fraction. In this case, the high altitude (800 km) means that the bounce path of many of the electrons will be entirely above 500 km and counted as trapped using this model. However, for burst longitudes where the magnetic field is strong, the particles will move closer to Earth as they drift, and those with smaller values of equatorial pitch-angle will be lost as they drift. Calculating the trapping fraction by identifying which particles are on closed drift shells produces a much smaller trapping fraction in this case than the approach using the 500k altitude atmosphere (the opposite of what we discussed in the previous paragraph). Furthermore, in this case, the higher-order moments represented by IGRF also affect the trapping fraction since the trapping fraction computed using IGRF 1960 is 2.5x smaller than that computed using an eccentric dipole.

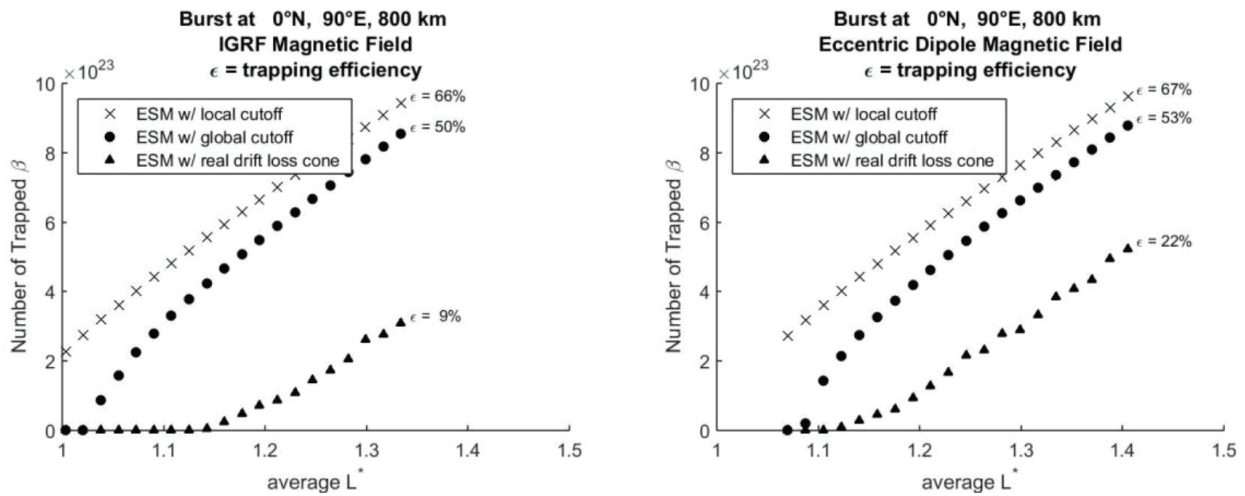


**Figure 3.** Total number of trapped electrons versus  $L^*$  using the eccentric dipole (right) and IGRF (left) magnetic field models, for a burst far from the South Atlantic Anomaly at 800 km altitude. Trapping fractions were computed using a) the local bounce loss cone with 120 km atmosphere (x), b) the local bounce loss cone with 500 km atmosphere (circle), and c) by identifying those electrons that are on closed drift shells (triangles).

## Conclusions

We have extended the Electron Source Model (ESM) so that it transports the fission fragment debris along a finite number of field lines intersected by the burst volume in the IGRF magnetic field model, whereas previously a less accurate centered dipole model was used. This initial population of electrons is transported to the point along the field line where the minimum value of magnetic field intensity is obtained and the number of electrons as a function of equatorial pitch-angle is tallied for each field line. We further computed the set of closed drift-shells in IGRF so that we could determine which electrons would be "permanently trapped," i.e., could drift entirely around Earth without encountering the atmosphere at 120 km. This population of particles is only a fraction of those particle whose bounce motion allows them to stay above 120 km altitude on the particular field line on which they were produced through radioactive decay, i.e., those particles that are "bounce-trapped."

The trapping fraction was computed using three different methods, which revealed that there can be substantial sensitivity of the trapping fraction to the latitude, longitude, altitude and field model that is used. The new methodology that computes permanently-trapped electrons using the IGRF produces larger trapping fractions than what is obtained using a centered dipole model with a 500 km atmosphere for burst longitudes that have comparatively small magnetic field strength, as in the South Atlantic Anomaly, whereas the new methodology produces lower trapping fractions for bursts at longitudes with strong magnetic fields. We conclude that proper consideration of the drift loss cone is important in computing the trapping fraction of betas produced by a high-altitude nuclear explosion.

In future work, we will use the mapping of the electrons onto closed drift-shells to produce an initial condition phase space density that can be evolved forward in time in response to interactions with naturally-occurring electromagnetic waves as modeled by the Dynamic Radiation Environment Assimilation Model 3D (DREAM3D), a Fokker-Planck diffusion code that we have used to model the natural radiation belts [9].

## Acknowledgment

The authors would like to thank DTRA for their continued support.

## References

- [1] J.A. Van Allen, "Spatial distribution and time decay of the intensities of geomagnetically trapped electrons from the high altitude nuclear burst of July 1962," in *Radiation Trapped in the Earth's Magnetic Field*, B.M. McCormac, Ed., Holland: D. Reidel Publishing Co., 1966, pp. 575-592.
- [2] M.M. Cowee *et al.*, "Initial Comparisons of the Los Alamos HANE Energetic Electron Source Model with HANE Test Data," *JRERE*, vol. 31-1, 2013.
- [3] J.G. Roederer and H. Zhang, *Dynamics of Magnetically Trapped Particles*, 2nd ed., New York: Springer, 2014.
- [4] G.S. Cunningham, "Radial diffusion of radiation belt particles in non-dipolar magnetic fields," *J. Geophysical Research: Space Physics*, vol. 121, no. 6, pp. 5149-5171, May 2016.
- [5] V.P. Shabansky, "Some processes in the magnetosphere," *Space Sci. Reviews*, vol. 12, no. 3, pp. 299-418, July 1971.
- [6] M.K. Öztürk and R.A. Wolf, "Bifurcation of drift shells near the dayside magnetopause," *J. Geophysical Research: Space Physics*, vol. 112, A07207, July 10, 2007.
- [7] R. Carter *et al.*, "Free anti-neutrino cross sections II. Experimental cross-section from measurements of fission fragment electron spectrum," *Physical Review*, vol. 113, Jan. 1959.
- [8] N.A. Tsyganenko, "A magnetospheric magnetic field model with a warped tail current sheet," *Planetary and Space Sci.*, vol. 37, no. 1, pp. 5-20, Jan. 1989.
- [9] W. Tu *et al.*, "Modeling radiation belt electron dynamics during GEM challenge intervals with the DREAM3D diffusion model," *J. Geophysical Research: Space Physics*, vol. 118, pp. 6197-6211, Oct. 2013.
- [10] W. Tu *et al.*, "Event-specific chorus wave and electron seed population models in DREAM3D using the Van Allen Probes," *Geophys. Res. Lett.*, vol. 41, pp. 1359-1366, March 5, 2014.